Improving signal-to-noise ratio of passsive seismic data with an adaptive FK filter

Chuntao Liang, Mike P. Thornton, Peter Morton, BJ Hulsey, Andrew Hill, and Phil Rawlins, Microseismic Inc.*

Summary

We introduce an adaptive FK filter to improve the signal to noise ratio of passive seismic data. This method integrates the unique geometry of surface seismic arrays and the distribution of microseismic events induced by hydraulic fracturing. Results from both synthetic and field data show that this technique significantly improves the visibility of microseismic events in the surface recorded data. Applied together with envelope stacking, this method can efficiently locate events with various focal mechanisms.

Introduction

Surface based seismic arrays have been successfully applied to numerous fracture monitoring projects [*Lakings et al*, 2005, *Duncan & Lakings*, 2006, *Abbott et al*, 2007, *Eisner et al*, 2008, *Williams-Stroud et al*, 2008, *Hulsey et al* 2009]. Microseismic events induced by hydraulic-fracturing generally have a low signal-to-noise-ratio (SNR). At the same time, polarity changes are very often observed for events with shear focal mechanism associated with faulting [*Williams-Stroud et al*, 2008]. *Eisner et al* [2008] and *Hulsey et al* [2009] used a matched filter method to improve SNRs and also to address the polarity reversal issue. In this study we implement another method, adaptive FK (AFK) filter, to improve the SNR of microseismic events. Used together with envelope or absolute amplitude stacking, this method also efficiently solves the polarity reversal issue.

Method

As illustrated by a 2D profile in Figure 1, the surface based monitoring array generally extends 4-6km in horizontal distance [*Duncan & Lakings* 2006] while the microseismic events induced by hydraulic fracturing are concentrated in a relatively small area (Frac Volume shown as a yellow box). As a result, apparent velocities (C) of primary waves generated by an event in the frac volume vary dramatically from one end of the array to another. For example, the apparent velocities are negative, positive and infinite for receivers on the left, on the right and above the event, respectively. To take advantage of this dramatic apparent velocity variation, an adaptive FK filter is devised to filter waves based on the estimated apparent velocity from receiver to receiver.

Based on Snell's Law:

$$p = \frac{1}{C} = \frac{\sin(\theta)}{V_{RMS}}, \qquad (1)$$

Where θ and V_{rms} are the incidence angle and root-mean-square velocity above the source, respectively, while p is the slowness (or dip). Note that dip changes continuously across the receiver above the event from left to right.

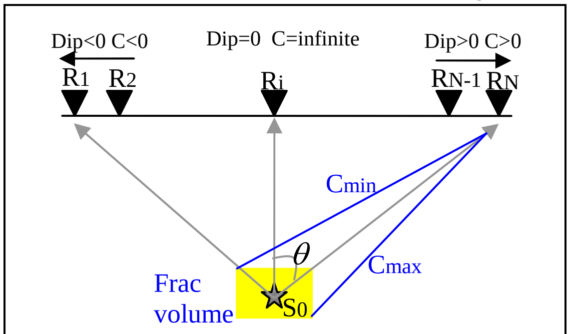

Figure 1: The concept of the Adaptive FK filter. Triangles and the star denote the receivers and microseismic event, respectively. The yellow box denotes the Frac volume where most of the Hydraulic Fracturing induced microseismic events occur. Two arrows mark the different directions of primary waves due to the relative locations of receivers and the event. For a given Frac volume, the minimum (Cmin) and maximum (Cmax) apparent velocity for each receiver can be estimated. C is apparent velocity and Dip=1/C.

For the 3D case, the seismic event is projected onto the vertical plane containing the receiver line and the incident angle is computed similarly as in Figure 1. For an estimated 3D frac volume, we compute the minimum and maximum apparent velocities for each receiver corresponding to a given velocity model (Figure 1), and the FK filter is applied to enhance waves traveling with Cmin<C<CMax.

Examples

We tested our technique using both synthetic and field datasets. The geometry of the synthetic experiments (Figure 2) is designed to mimic the typical surface based monitoring array. Both dip-slip and strike-slip events are commonly observed in hydraulic frac monitoring [*Williams-Stroud*, 2008]. Non-shear events (explosive or contractive) may also coexist with shear events. Therefore, we tested both non-shear and shear focal mechanisms as shown in Figure 4 and Figure 5, respectively. The synthetic microseismic events have SNRs from 0.1 to 1.1 and are almost invisible on the original waveforms (Figure 3a). After applying the AFK filter (Figure 3b), events with SNRs larger than 0.6 (near and after 30 seconds) become visible. Figure 4 shows the stacked traces of the original waveforms (4a-4b) and their corresponding envelopes (4d-4e). All events can be identified on the stacked waveforms before (4a) and after (4b) applying AFK filter even though some events are invisible on the waveforms in Figure 3.

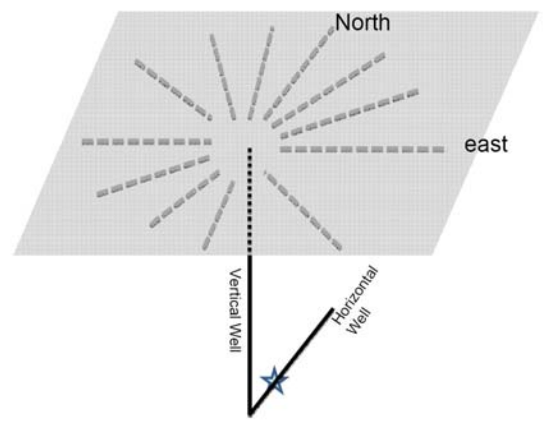

Figure 2: Geometry for synthetic examples. 100 receivers with a uniform spacing of 20 meters are placed along each of the 12 arms of the star array. The horizontal well is parallel to the north arm and is about 1.5km deep. 11 seismic events are placed on horizontal well and are 50m away from the heel of the vertical well (star). RMS velocity above the source is 2km/s.

Figure 4c compares the SNRs of the stacked waveforms. The SNRs of all events on the stacked waveforms are consistently higher for AFK filtered waveforms (Red) than un-filtered waveforms (Black), the SNR improvement is about 10-20%.

To address the polarity changes due to a shear source mechanism, the envelope stack (Figure 4d and 4e) may be preferred over the waveform stack. Using the envelope stack, 10 (of 11) events (SNR>=0.2) are visible on the stacked envelope with AFK filtering (Figure 4e), while only 7 events (SNR>=0.5) are visible without using AFK filtering (Figure 4d). Note that for both cases, fewer events can be identified on stacked envelopes than the stacked waveforms. This suggests that waveform stack is preferred when focal mechanisms of all events are explosive or contractive.

For strike-slip sources (Figure 5), due to the cancellation of reversed wave polarity, none of the 11 events are visible on the stacked waveforms, with (Figure 5b) or without (Figure 5a) the AFK filtering. On the other hand, 9 and 5 events can be identified on the stacked envelopes of the AFK-filtered waveforms (Figure 5e) and original waveforms (Figure 5d), respectively. In this case, the AFK filter increases the number of events being located.

The adaptive FK filter is also applied to the field data from the Delaware Basin in west Texas as shown in Figures 6 and 7. On Figure 6a, two microseismic events near 275 (E2) and 282 (E1) seconds are weakly visible between receiver 760 and 820. After the AFK filtering on Figure 6b, signals of these two events are significantly enhanced, especially the signals of receivers between 740 and 760. In addition, two more events are observed on Figure 6b near 260 (E4) and 271 (E3) seconds while they are invisible on Figure 6a. Interestingly, all four events cannot be identified from the stacked waveforms with (7b) or without (7a) applying the AFK filter. This suggests that the focal mechanisms of these events are most likely shear, or at least not purely explosive or contractive. As a result, reversed polarity cancels during the waveform stacking. On the other hand, three events near 271, 275 and 282 seconds can be identified on the stacked envelope easily for both before (7d) and after (7e) AFK filtering. The amplitude of the event near 260 seconds, however, is

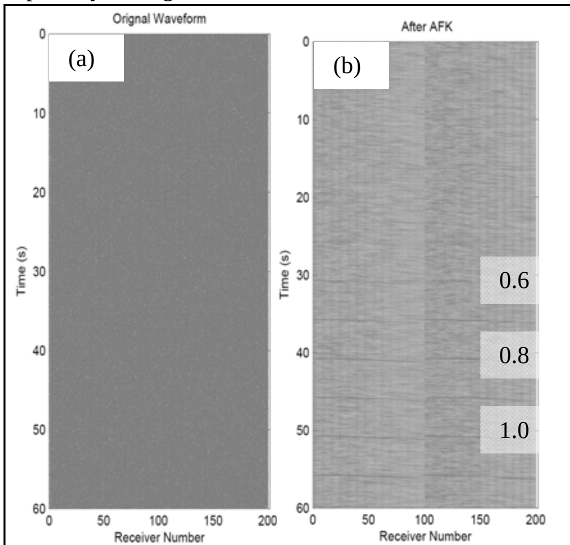

Figure 3. (a) Synthetic waveforms of the first 200 receivers: background noise (amplitude between -1 and 1) mixed with 11 seismic events. The waveform peak of the 11 seismic events are successively increasing from 0.1 to 1.1 with a 0.1 interval and the corresponding orign times are from 5 seconds to 55 seconds with an interval of 5 seconds. Thus, the signal-to-noise-ratio (SNR) of the 11 events are from 0.1 to 1.1; and (b) the waveform after applying the adaptive FK filter. The numbers on the right are the SNRs of the corresponding events.

indistinguishable from the background noise on Figure 7d while it is obviously over the background noise level on Figure 7e. Figure 7f shows that the AFK filter significantly improves SNRs of the stacked envelopes, especially the event near 260 seconds which can only be identified when AFK filter is applied (red).

synthetic and field data show that the AFK filter significantly increases the visibility of microseismic events. It also increases the SNRs of stacked waveforms by 10-20% and SNRs of stacked envelope by more than 2 times. The AFK-filtered waveforms may be used together with the matched filter to locate events [*Eisner et al* 2008, *Hulsey et al* 2009], or to identify fault geometry [*Williams-Stroud et al*, 2008] and other studies.

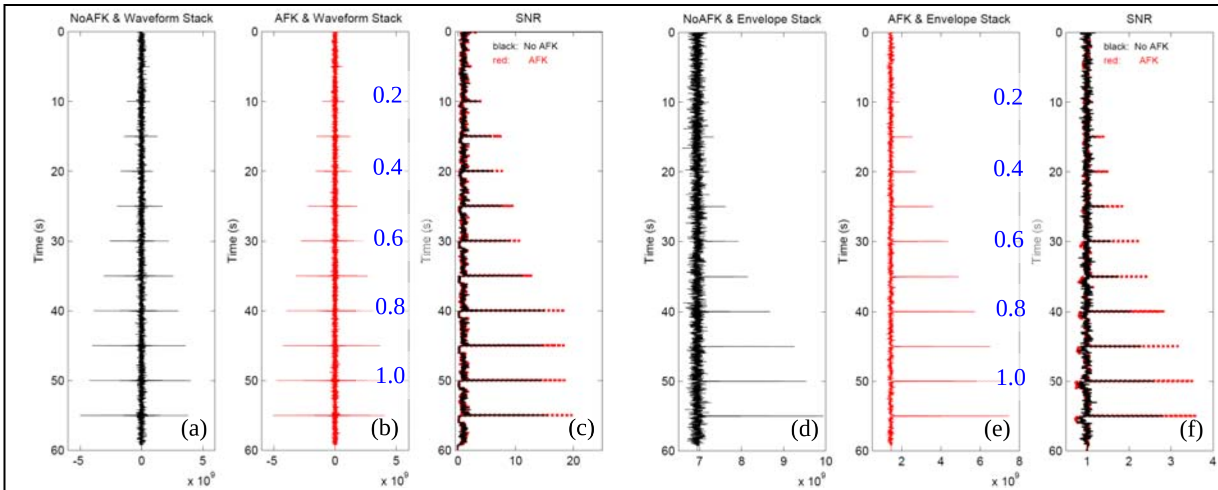

Figure 4: Waveform stacking (a-c) and envelope stacking (d-f). For the given source location and velocity model, waveforms are shifted based on travel time and are stacked. (a) and (b) are stacked traces of waveforms before and after applying AFK, respectively and (c) compares the signal-to-noise-ratio (SNR) of (a) and (b). The SNR is defined as the ratio between the root-mean-square amplitude of the time windows 50ms after and 1s before one time point. (d)-(f) are similar to (a)-(c) but for envelope stacking. Each pulse correspods to an event as described in Figure 3. The numbers in blue color are the SNRs of the corresponding events. Note the difference between the SNR of events in blue text and the SNR of stacked traces 4c and 4f.

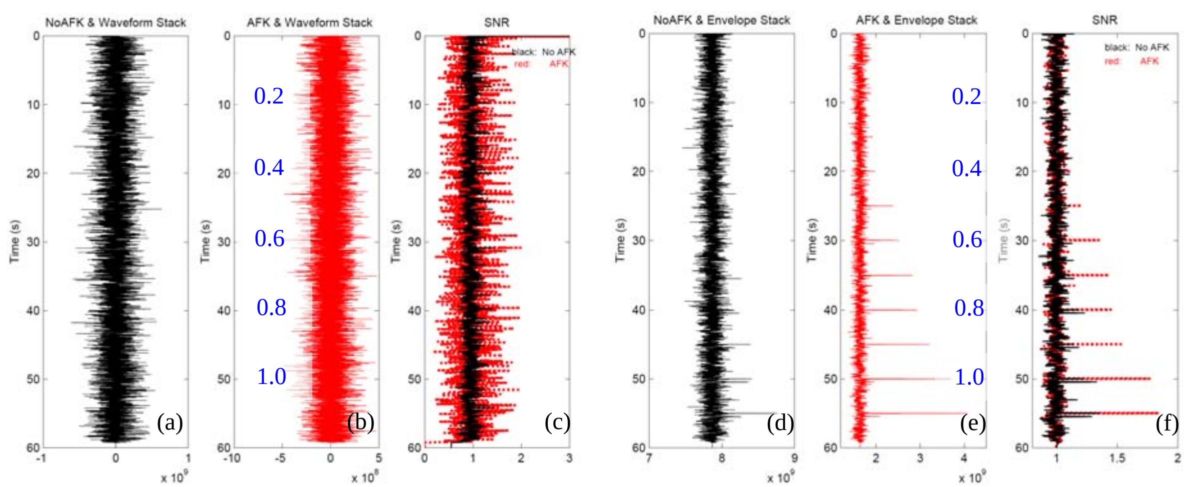

Figure 5: Similar to Figure 4, but source mechanisms for all 11 events are strike-slip with a strike of 15 degree from north.

Discussions and Conclusions

We have developed a new adaptive FK filter (AFK) method to improve the signal-to-noise-ratio (SNR) of microseismic events induced by hydraulic fracturing. Both

For the case when all events are either explosive or contractive such as the perforation and string shot (the case shown in Figure 4), normal waveform stacking works well to illuminate microseismic events. Envelope stacking, on the other hand, fails to illuminate some small magnitude events.

However, source mechanisms of microseismic events induced by hydraulic-fracturing are often very complicated depending on the stress and strain history and the existing structure. Both explosive sources and shear sources associated with different fault geometries and slip vector (strike, dip and rake) may coexist. In this case, the envelope stacking is thus preferred. As shown in the synthetic experiments (Figure 5) and field data (Figure 7), the AFK filtering method can significantly improve SNRs of events on the stacked envelopes. Therefore, the AFK filtering together with envelope stacking is strongly recommended in this case. It's also worth mentioning that the envelope stacking may be replaced with stacking the absolute value of waveforms to deal with polarity variation issue. The same conclusions can be made for the absolute value stacking as the envelope stacking.

Acknowledgments

We thank Microseismic Inc. for the permission to publish this work. We also thank Leo Eisner, Peter Duncan and Sherilyn Williams-Stroud for reviewing this abstract and their invaluable suggestions.

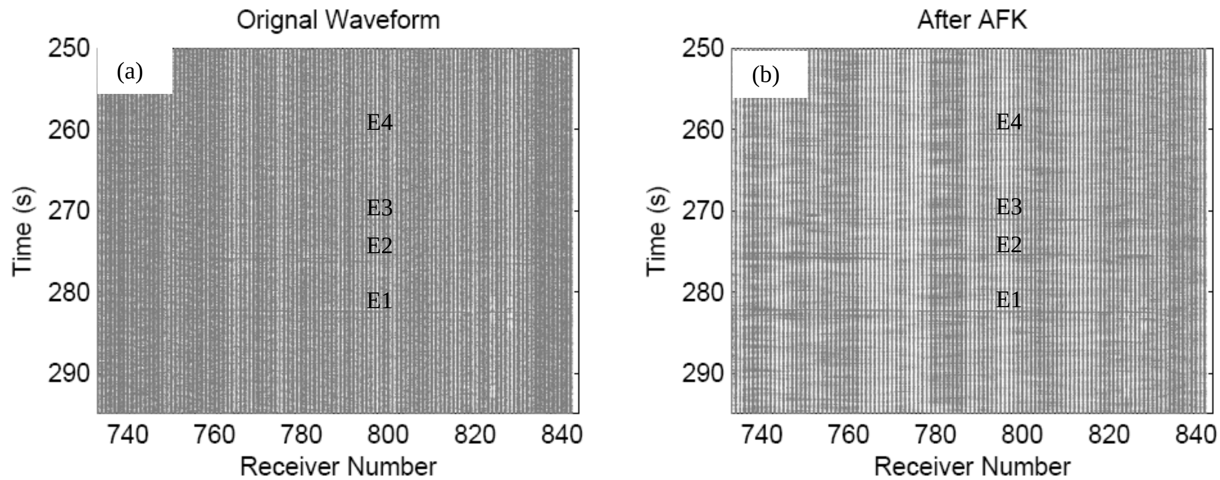

Figure 6: Before (a) and after (b) AFK-filtered waveforms from the Delaware Basin dataset. E1 to E4 mark the four events identified on the stacked envelopes in Figure 7.

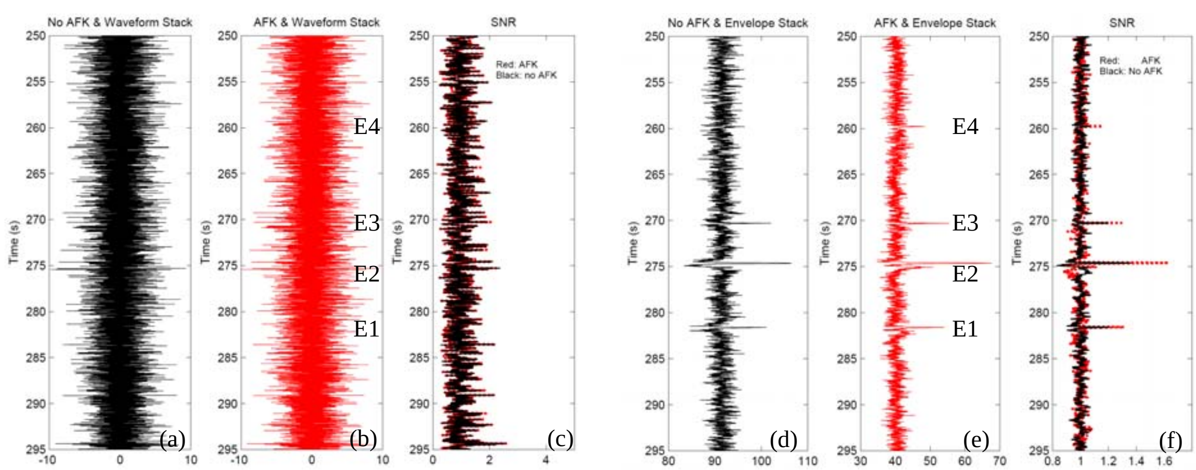

Figure 7: Similar to Figure 4, but for waveforms from field data as shown in Figure 6.

EDITED REFERENCES

Note: This reference list is a copy-edited version of the reference list submitted by the author. Reference lists for the 2009 SEG Technical Program Expanded Abstracts have been copy edited so that references provided with the online metadata for each paper will achieve a high degree of linking to cited sources that appear on the Web.

REFERENCES

Abbott, D., C. Neale, J. Lakings, L. Wilson, J. C. Close, and E. Richardson, 2007, Hydraulic fracture diagnostics in the Williams Fork Formation, Piceance Basin, Colorado, using surface microseismic monitoring technology: Rocky Mountain Oil & Gas Technology Symposium: Society of Petroleum Engineers, 108142.

Duncan, P., J., and Lakings, 2006, Microseismic Monitoring with a Surface Array, 67th Conference and Exhibition, EAGE, Extended Abstracts.

Eisner, L. D., Abbott, W. B. Barker, J. Lakings, and M. P. Thornton, 2008, Noise suppression for detection and location of microseismic events using a matched filter: 78th Annual International Meeting, SEG, Expanded Abstracts, 1431–1435.

Hulsey, B. J., L. Eisner, M. P. Thornton, D. Jurick, 2009, Application of relative location technique from surface arrays to microseismicity induced by shale fracturing, 79th Annual International Meeting, SEG, Expanded Abstracts.

Lakings, J. T., P. M. Duncan, C. Neale, and T. Theiner 2005, Surface based microseismic monitoring of a hydraulic fracture well simulation in the Barnett shell: 75th Annual International Meeting, SEG, Expanded Abstracts, 605–608.

Williams-Stroud, S., 2008, Using microseismic events to constrain fracture network models and implications for generating fracture flow properties for reservoir simulation: Shale Gas Production Conference, SPE, 119895.